Journal of Medical Radiation Sciences

Open Access

ORIGINAL ARTICLE

Effect of patient size on image quality in radiotherapy kV planar verification imaging: a phantom study

Sara Chan, BMedRad (Hons),[1,2] Eileen Giles, MHSc (MRS), BApSci (RT), FASMIRT,[1] Lyndal Newmarch, BMedRad, [2] & Michala Short, BMedRad (Hons), PhD[1]

[1]Centre for Translational Cancer Research, UniSA Cancer Research Institute and School of Health Sciences, University of South Australia, Adelaide, South Australia, Australia

[2]Department of Radiation Oncology, Royal Adelaide Hospital, Adelaide, South Australia, Australia

Keywords
image interpretation, image-guided radiotherapy, phantoms, waist circumference

Correspondence
Michala Short, Centre for Translational Cancer Research, UniSA Cancer Research Institute, University of South Australia, GPO Box 2471, Adelaide, SA 5001, Australia. Tel: +61 8 8302 2089; Fax: +61 8 8302 1818; E-mail: Michala.Short@unisa.edu.au

Received: 17 April 2019; Revised: 8 August 2019; Accepted: 10 August 2019

J Med Radiat Sci **67** (2020) 34–42

doi: 10.1002/jmrs.355

Abstract

Introduction: This study aimed to determine a maximal pelvic separation and waist circumference in pelvic patients to guide radiation therapists in acquiring kilovoltage (kV) planar images of acceptable quality for treatment verification. **Methods:** A pelvic anthropomorphic phantom modified with different bolus thicknesses was imaged at various default kV exposure settings. Radiation therapists rated image quality and acceptance/rejection of these images for treatment verification. **Results:** Sixteen radiation therapists participated in the study. Image quality was inversely proportional to phantom size. AP and lateral kV images were acceptable for treatment verification up to a waist circumference of 143 cm. **Conclusions:** Exposure settings for kV image verification of large patients should be individualised to avoid unnecessary patient radiation dose through repeated imaging.

Introduction

Image verification and the use of image-guided radiotherapy (IGRT) underpin treatment success.[1] Cone-beam computed tomography (CBCT) is one option for image verification, with implementation undergoing a surge in Australia and New Zealand. Recent 2015–2016 surveys show that CBCT was available in 97% of Australian departments[2] and in 86% of New Zealand departments[3] compared with 8% of departments in this region having CBCT just a decade ago.[4] Despite being available in almost all departments, CBCT has not replaced other image verification modalities, with kilovoltage (kV) planar imaging being the second most common imaging tool used in IGRT.[2]

Since obesity prevalence in Australia is on the rise,[5] establishing image verification protocols for large patients is becoming an important issue. Several image verification guidelines and reports have been published nationally and internationally.[6–9] Except for the study by Wood et al.,[6] all other studies recognise the need to individualise imaging protocols, but fall short of recommending the specific image acquisition parameters and exposure factors to be followed. It is likely that many RT centres have locally developed protocols for obese patients; however, as these are not publicly available, it is not possible to comment on their content.

Definitions of obesity are varied, with the body mass index (BMI; weight in kilograms divided by height in metres squared) being the most widely known. According to BMI categories, a BMI >30 corresponds to obesity.[10] Although BMI is commonly used, its main limitation is not being able to account for body fat distribution, which may explain the lack of association observed between BMI and intra-fraction motion in patients receiving radiotherapy for prostate cancer.[11,12] Therefore, to overcome the limitations of BMI, an alternative metric called ‘waist circumference’ in centimetres was proposed by the Australian Institute of Health and Welfare, where a waist circumference >94 cm in men and 80 cm in women is associated with an increased risk of chronic disease.[13]

Modern linear accelerators allow for a number of different image acquisition settings. The kilovoltage (kV) X-ray imaging system on a Varian Trilogy® iX linear accelerator enables the user to individualise exposure parameters to the patient, including selections for anatomical site, projection and patient size (Table 1). For very large patients, exposure parameters can be manually adjusted by the radiation therapist (RT) to improve image quality if the default exposures prove insufficient;[14] however, this practice depends on the clinical judgement and experience of the RT acquiring the image.[15] Ideally, RTs would refer to a protocol or guidelines to assist with increasing exposure settings for very large or obese patients, as trial-and-error may result in repeated imaging and therefore higher patient dose. Additionally, longer time for patient set-up and image acquisition increases the chance of intra-fraction motion and subsequently impacts on patient throughput and department workflow.

The literature is consistent in reporting that larger patient separations result in poorer signal-to-noise ratio[16–20] an objective measure of radiographic image quality – however, image verification during IGRT is a subjective process and so objective image quality measures in a radiotherapy setting are less often referred to. At times, even if the overall image quality is poor due to inadequate exposure settings, RTs observe enough anatomical information or use visual aids such as implanted fiducial markers to perform image verification thus avoiding repeated imaging and extra patient dose. If it was possible to individualise exposure settings based on patient's actual size, such as their waist circumference or their separation, there would be a greater likelihood of producing the initial verification images of an acceptable quality resulting in fewer instances of repeated imaging and thus less dose and a shorter treatment time. A waist circumference measurement can be obtained by RTs at CT simulation with a tape measure, or an approximate waist circumference can be calculated from patients' CT data using the maximum anterior–posterior (AP) and lateral half-separations inputted into an elliptical equation.[21]

Table 1. Default exposure parameters for pelvis imaging on a Varian Trilogy® iX linear accelerator

Acquisition setting	Tube voltage (kilovolts peak)	Tube current (milliamperes)	Exposure time (milliseconds)	Current-exposure product (mAs)
AP normal	75	200	50	10
AP large	75	200	80	16
Lateral normal	105	200	400	80
Lateral large	120	200	630	126

In the absence of an imaging protocol for very large patients in a large public radiotherapy department, the aim of this study was to determine the AP and lateral separations, as well as a maximum waist circumference threshold that would result in acceptable kV image quality as subjectively rated by RTs. This would then provide an evidence base on which to develop a kV image verification protocol with associated image exposure parameters tailored for obese patients.

Methods

This research was approved by Ethics Committees at the Royal Adelaide Hospital (RAH) (HREC/15/RAH/443) and the University of South Australia (ID: 0000034251) with all participants providing written informed consent to participate. The study was conducted in two parts: (1) creation of an image verification dataset using a phantom with the addition of bolus material to simulate different patient sizes, and (2) image quality assessment performed by RTs.

Image dataset

To create the image dataset, an anthropomorphic phantom of an average adult male pelvis (encompassing the third lumbar vertebra to the upper quarter of femurs) was first enclosed in a tissue equivalent wax block (Dickson™ paraffin wax, bees wax and other waxes). Additional bolus sheets (Superflab™) of varying thicknesses were then attached to the front, back and both sides as shown in Figure 1. As the quantity of bolus available was limited, different thicknesses were separately built in the plane that was to be imaged, rather than circumferentially.

The phantom's AP and lateral separations (without bolus) were 22.4 and 33.3 cm, respectively, and these were referred to as Size 0. Three additional phantom sizes 1, 2 and 3 were created by progressively attaching 4, 8 and 12 cm slabs of Superflab™ to the front, back and both sides of the phantom as shown in Table 2. The largest size (phantom plus 12 cm in all directions, approximate waist circumference 169 cm) was based on the largest patient clinically observed at the RAH. Waist circumferences were estimated using equation 1, which calculates the approximate perimeter of an ellipse by using the measurement of the long and short axes a and b, where a and b were defined as the maximal AP and lateral half-separations.[21]

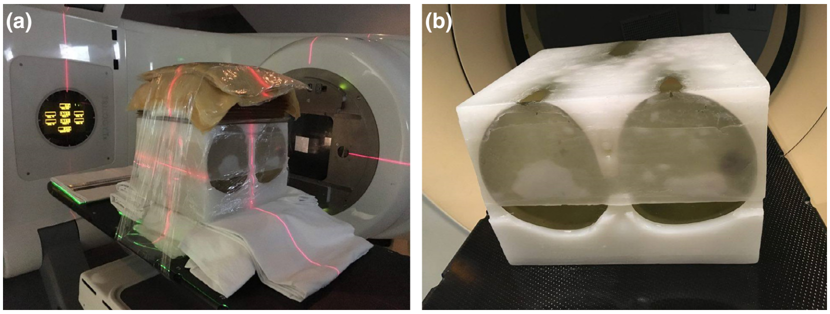

Figure 1. (A) Phantom–bolus assembly set-up for anterior–posterior image acquisition. NB: bolus sheets were added at anterior and posterior; gantry not yet in position; (B) Phantom enclosed in wax block to minimise air gaps.

Table 2. Phantom size parameters

Phantom size	Image projection	Separation (cm)	Equivalent waist circumference (cm)[1]
Size 0 (no bolus)	AP	22.4	89
	Lateral	33.3	
Size 1	AP	30.5	117
	Lateral	42.8	
Size 2	AP	39	143
	Lateral	51	
Size 3	AP	46.5	169
	Lateral	60	

[1]Calculated using equation 1 as bolus was not applied circumferentially.

Equation 1. Perimeter of an ellipse

$$p \approx 2\pi\sqrt{\frac{a^2 + b^2}{2}} \quad (1)$$

Prior to image acquisition, imager and detector warm-up was performed to ensure consistent panel response. In total, sixteen kV X-ray images were acquired as shown in Figure 2 using the Varian Trilogy® iX kV imaging system: each phantom size was imaged with four previously described vendor-specific image acquisition settings (Table 1). The source to axis distance (100 cm) and vertical distance from isocentre (50 cm) remained constant throughout. AP images were acquired at a field size of 15.0 cm × 12.5 cm and lateral images at 12.5 cm × 12.5 cm to mirror clinical practice for typical pelvic radiotherapy. Appropriate radiation safety procedures were followed by the first author under the supervision of all co-authors. Acquired kV images were then saved electronically in a Tag Image File (.TIF) format to avoid compression artefacts. Figure 3 shows examples of several of the acquired images.

Instrument validity was measured by first acquiring a CT of the phantom–bolus assembly (Philips Brilliance Big Bore CT, Philips Healthcare, Amsterdam, Netherlands), importing the dataset to Pinnacle[3] treatment planning system (version 9.10, Philips Medical Systems, Amsterdam, Netherlands), profiling the electron densities of the phantom, wax and bolus sheets and comparing these to established values.[22] Soft tissue densities were 1.1 g/cm^3, bone was 1.7 g/cm^3 and adipose tissue was 0.9 g/cm^3. As these parameters were deemed to have good approximation to normal human tissue densities, the resulting kV images of the phantom were considered valid for use in this study.

Image quality assessment

RTs from a single department were recruited to participate via a flyer containing study information. To be eligible, RTs required full qualification, registration and be currently practising, as well as credentialled in image verification and at least 1 year experience in treatment verification.

Each RT attended an image quality assessment session lasting approximately 15–20 min. The session was conducted in a quiet room of the department with the first author present and facilitating the image assessment. All environmental factors such as lighting were kept consistent between participants. The specially acquired phantom images were displayed one at a time on a Compaq LA 1956x monitor (Hewlett-Packard Company, Palo Alto, CA) with Picture Manager software (Microsoft Corporation, Redmond, WA), and the RT was asked to complete a short questionnaire after viewing each image. The questionnaire was developed specifically for this study and included the following questions: (1) image quality rating (Likert scale, 1 = very poor, 2 = poor, 3 = reasonable, 4 = good, 5 = very good); (2) would the RT accept the image for treatment verification? (Yes/No); and (3) what post-processing filters the RT would apply to improve image quality (multiple-choice showing all possible filter settings for example 'dynamic filter',

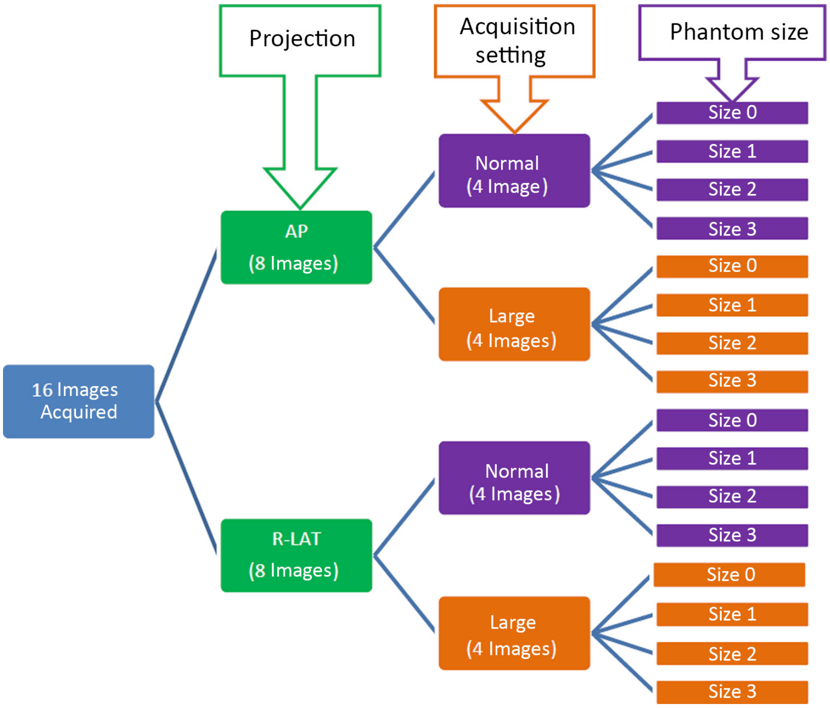

Figure 2. Summary of image projections and acquisition settings. AP, anterior–posterior; R-LAT, right lateral.

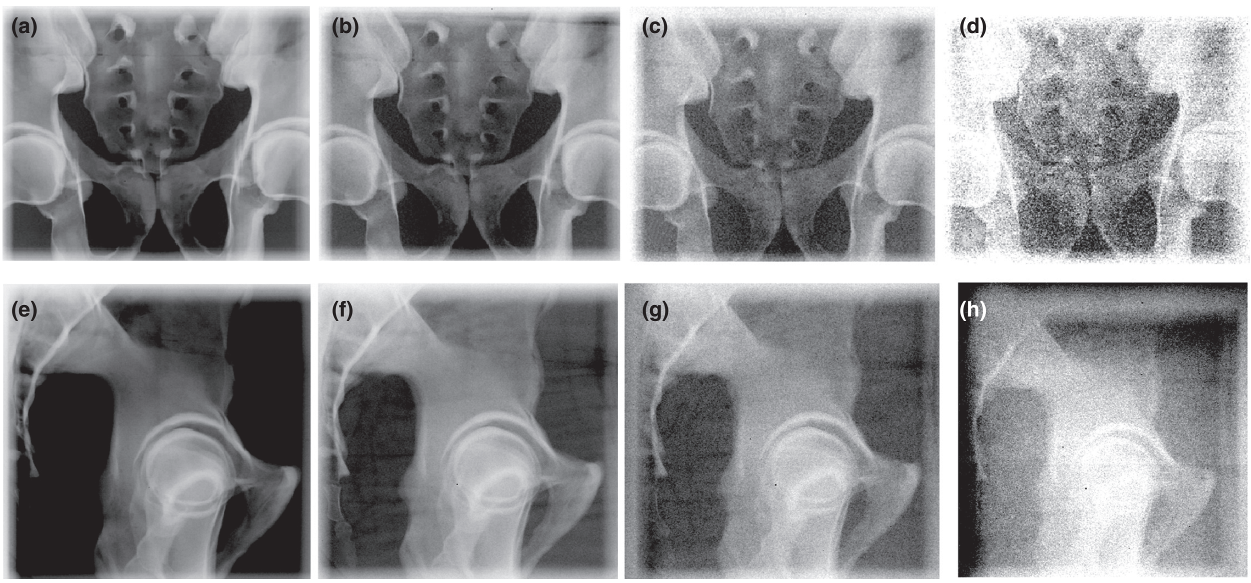

Figure 3. Exemplars of images acquired at different phantom sizes, top panel anterior–posterior images, bottom panel right lateral projections. (a) Size 0, (b) Size 1, (c) Size 2, (d) Size 3, (e) Size 0, (f) Size 1, (g) Size 2, (h) Size 3.

'contrast low', 'optimised' as well as 'no filter' as an option). To measure the consistency of RTs' image quality ratings, intra-observer reliability was conducted by adding one duplicate image to the set, which the participants were blinded to.

Data analysis

Descriptive statistics were used to summarise image quality ratings (median and interquartile range) and image acceptances (frequencies). Data were presented as box plots to show the spread of image quality ratings about the median for all phantom sizes. The effect of the 'normal' and 'large' image acquisition settings on the image quality ratings for the same phantom size was also compared. Correlations between phantom sizes and image quality ratings were calculated using Spearman's Rho correlation coefficient at a significance level of $\alpha = 0.001$. The odds of accepting images for each phantom size, projection and acquisition setting were calculated. The maximum phantom size beyond which images were considered to be too poor for accurate image verification was determined using the Cochran's Q test ($\alpha = 0.05$) to test whether image acceptance rates were significantly different between the four phantom sizes. If a significant difference was found, the McNemar test was used to pinpoint the pair of phantom sizes which were significantly different. Intra-observer and inter-observer reliability of image quality ratings were tested using the Wilcoxon signed-rank test and the intra-class correlation coefficient (ICC), respectively. All analyses were conducted using the IBM Statistical Package for the Social Sciences (SPSS) software version 21 (IBM Corporation, Armonk, NY).

Results

Sixteen participants gave written informed consent to participate, with data collection occurring March–May 2016. Table 3 shows a summary of participants' characteristics.

For intra-observer reliability, the Wilcoxon signed-rank test showed no significant differences at $\alpha = 0.05$, indicating that image quality ratings given for the first and the duplicate image were similar and RTs judged the quality of images in a consistent manner. For inter-observer reliability, the ICC for image quality ratings was $R = 0.81$ with a 95% confidence interval of 0.69–0.91, indicating that RTs had excellent agreement and rated image quality similarly to each other.

Table 3. Participant characteristics, $n = 16$

Characteristic	Frequency n (%)
Gender	
Female	9 (56)
Male	7 (44)
Months since last image review	
Reviewing daily	9 (56)
≤6 months	4 (25)
>6 months	3 (19)
Senior radiation therapist[1]	
Yes	7 (44)
No	9 (56)

[1]Defined as >5 years clinical experience plus demonstrating additional capabilities.

Image quality and phantom size

A strong, statistically significant inverse relationship was found between phantom size and image quality ratings, with all Spearman R coefficients greater than -0.712 at $p < 0.001$, as shown in Table 4. Figure 4 illustrates these relationships using box plots.

Image acceptance and phantom size

Comparisons were undertaken to determine the odds of accepting images for treatment verification between phantom sizes. For all image projection and acquisition setting combinations, the odds of accepting an image were greater than the odds of rejecting, up until phantom Size 2. At Size 3, the odds of accepting became less than the odds of rejecting. Therefore, the threshold size for acceptable image quality was between phantom Sizes 2 and 3. These results are shown in Table 5. The difference in acceptance rates between the two sizes was also found to be statistically significant using the Cochran's Q test and McNemar tests with all $P < 0.05$. When converting these sizes to equivalent waist circumferences, the threshold fell between a waist circumference of 143 and 169 cm. Up to a waist circumference of 143 cm, the images acquired using the default parameters were acceptable for treatment verification, whereas at 169 cm, RTs were less likely to accept the verification image.

Post-processing

Data on post-processing were analysed descriptively using percentages. For all image projections and acquisition setting combinations, the proportion of RTs choosing 'no filter' decreased from 60–87% at Size 0 to 0–13% at Size 3. For phantom Sizes 0–2, the 'sharpen high (PV)' filter was the most common selection among RTs. Other selections made by fewer RTs included 'contrast high (PV)', 'contrast low (PV)', 'smooth', 'dynamic filter' and

Table 4. Relationship between phantom size and image quality

Spearman's rho correlation coefficient (R) ($n = 64$ images, two-tailed, $\alpha = 0.001$)

Projection	Acquisition setting	R	p-value
Anterior–posterior	Normal	−0.891	<.001
	Large	−0.887	<.001
Right lateral	Normal	−0.712	<.001
	Large	−0.728	<.001

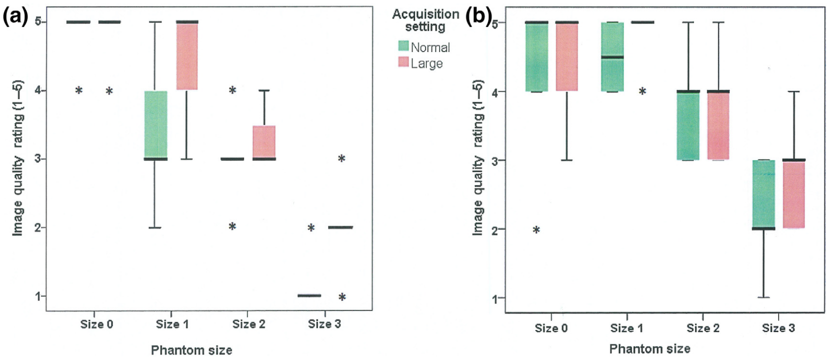

Figure 4. Phantom size versus image quality ratings. (A) Anterior–posterior; (B) right lateral. Image quality: 1 = very poor, 2 = poor, 3 = reasonable, 4 = good, 5 = very good. Thick horizontal lines represent median, thin horizontal lines represent the maxima and minima, shaded boxes are interquartile ranges, asterisks indicate outliers.

Table 5. Odds of accepting or rejecting an image at each phantom size, projection and acquisition setting

	Projection, acquisition setting			
Phantom size	AP, normal	AP, large	Lateral, normal	Lateral, large
	Accept: Reject			
0	15:1	15:1	14:1	13:3
1	11:5	15:1	16:0	15:1
2	12:4	14:2	13:3	13:3
3	0:16	6:10	5:11	9:7

'optimized'. Seven per cent of RTs opted to adjust the grey scale of the image with and without the 'sharpen high (PV)' filter, while another 7% opted to retake the image with different exposure factors for Size 3 phantom images.

Discussion

This study evaluated RTs' subjective ratings of image quality and resultant image acceptance of planar kV imaging used in image verification for a range of simulated patient sizes. To the authors' knowledge, this is the first study that evaluated the associations between RTs' decision-making in IGRT and varying waist circumferences under a range of kV image acquisition conditions available on a modern linear accelerator. A key strength of this study was the creation of a controlled, study-specific image dataset and its use in a process that mirrored RTs' clinical decision-making during kV image verification.

Our main findings showed that as patient size increased the quality of kV images decreased. More specifically, a threshold for waist circumference was found to be between 143 and 169 cm, as at phantom Size 3 there was a much greater likelihood of needing to repeat an image, as evidenced by RTs' low acceptance rates of images beyond this size. One exception to this was the marginally higher acceptance rate at the right lateral, large acquisition setting for phantom Size 3 (9 acceptances and 7 rejections). This observation may have been due to the highest exposures contained within this acquisition setting. Another result that warrants discussion was the variability in image quality observed for phantom Size 1 between the AP normal and large acquisitions (Fig. 4), where the median image quality was 3 (reasonable) at the normal setting and 5 (very good) at the large setting. The large acquisition setting had an increase of 30 milliseconds in the exposure and this small increase appeared to translate to a substantial increase in the perceived image quality. Since phantom Size 1 corresponded to an average-sized patient, this finding highlights the importance of selecting appropriate acquisition settings for any patient size.

It is well known that objective image quality can be defined by the degree of noise, contrast and/or spatial resolution and that when kV X-rays pass through a larger volume of tissue more X-rays are absorbed and scattered inside the patient with fewer photons reaching the detector, resulting in noisier, low contrast images.[18–20,23,24] Furthermore, since the photoelectric effect is the predominant effect for kV X-rays interacting with matter regardless of patient size, most of the radiation dose is deposited close to the skin surface which may decrease the image quality.[25] Accordingly, this was confirmed by RTs' subjective image quality ratings which showed worsening quality with increasing phantom size. While this process was performed individually rather than in pairs as would be the case in clinical practice, we still observed very high intra-class correlation coefficients among the 16 RTs, showing there was excellent agreement regarding image quality ratings.

A point of difference in our study was the addition of a follow-up question on the acceptability of a given image for treatment verification. This allowed us to gain insight into RTs' subjective clinical decision-making which has direct implications to clinical practice. We found that for patient separations between 39–46.5 cm in the AP direction and 51–60 cm in the lateral direction, the resultant image quality was deemed unacceptable for accurate treatment verification. These separations were equivalent to waist circumferences between 143 and 169 cm. The recommendation based on this finding is that patients exceeding these separation and waist circumference thresholds should have their exposure settings individualised by increasing the peak kilovoltage setting (kVp) and the tube current-exposure time product (mAs)[19] thus reducing the need for repeated imaging.

With improvements in technology over time, it is imperative that clinicians keep up-to-date with various tools and features available in newer equipment as well as across different vendors. One such development is the inclusion of a 'Pelvis Obese' default acquisition setting for CBCT acquisition on Varian TrueBeam® linear accelerators. A recent study conducted in the United Kingdom developed a CBCT protocol that took into account variations in pelvic size (small, medium, large and extra-large) and included corresponding exposure parameters that balanced image quality with minimum required patient dose.[6] Other software features such as post-processing filters should also be evaluated carefully. A notable finding in this study was the lack of consistency among participants regarding the post-processing filters that they would recommend as beneficial in improving image quality. Future work should investigate which filters provide the most 'gain' in terms of enhancing kV image quality.

The limitations of this study warrant discussion. First, the phantom–bolus assembly was not circumferential and we were unable to completely eliminate air gaps between the wax block and the bolus sheets. As such, this did not authentically represent patient anatomy. Ideally, snug-fitting bolus rings of different thicknesses would have been used to mould around the phantom similar to a study by Shindera et al.[26] thus enabling both CBCT and planar image acquisition. However, as there was only a defined quantity of bolus material available on loan, the set-up was limited to building the bolus thickness in the planes corresponding to beam paths for planar imaging. Second, the process of image verification was performed by RTs individually and on screenshots of the images, rather than with a colleague and with the benefit of full functionality in post-processing filters and additional matching tools, as would be the usual clinical practice. Finally, we were unable to investigate the effect of implanted fiducial markers on image acceptance in this study, however, recommend this for future research. In view of these limitations, the findings should be interpreted with a degree of caution.

As well as the aforementioned investigation into the value post-processing filters and fiducial markers offer in terms of image enhancement, future research into the default exposure settings as set by linear accelerator manufacturers should be undertaken for large patients as well as for all other default settings. During the creation of our image dataset, we experimented with acquiring images of the smallest phantom (Size 0, no bolus) at much lower exposure times than the default. For example, at surprisingly, low exposures (50% reduction in mAs for the normal AP (5 mAs compared with default 10 mAs) and 75% reduction in mAs for the normal lateral (20 mAs compared with default 80 mAs)) the kV images produced were deemed to be of acceptable quality for image verification. While doses from IGRT are very small in comparison with treatment doses, extra dose from imaging is not completely negligible and should follow the As Low As Reasonable Achievable (ALARA) principle.[27]

Any radiotherapy imaging protocol should be developed within a multi-disciplinary team and in accordance with published guidelines[1,9] with imaging dose balanced against clinical benefit achieved from extra imaging and the risk of inducing second malignant neoplasms.[1] This study provides a simple measure that can be taken at CT simulation and incorporated into an image verification protocol for large patients. A protocol like this could have wide-reaching benefits. For patients, it would offer reduced dose if repeated imaging is avoided and therefore decreased risk of intra-fraction motion contributing to improved treatment success. For departments, this implementation may improve efficiency by streamlining patient throughput.

Conclusion

Image quality when rated by RTs was inversely proportional to phantom size. Beyond a pelvic AP separation of 46.5 cm, lateral separation of 60 cm and the corresponding waist circumference of 169 cm, RTs deemed the image quality to be unacceptable for use in kV image verification. These results may inform size appropriate image exposure selection for larger pelvic patients who are representative of a subset of radiation therapy patients in Australia.

Acknowledgements

The authors acknowledge the following people who assisted in this work: Ms Sonya Stephens and Ms Kanan Sharma for their guidance with ethics approval matters, Mr John Schneider for his assistance with manufacturing the wax block materials, JelProducts (NSW) Pty. Ltd. for the loan of Superflab™ sheets during the data collection phase, to all RAH Radiation Oncology staff for their support and to all radiation therapists who volunteered their time to take part.

Conflict of Interest

The authors declare no conflict of interest.

References

1. Tiong A, Lao L, MacKean J, Goonetilleke M, Kron T. Faculty of radiation oncology position paper on the use of image–guided radiation therapy. *J Med Imaging Radiat Oncol* 2016; **60**: 772–80.
2. Batumalai V, Holloway LC, Kumar S, et al. Survey of image-guided radiotherapy use in Australia. *J Med Imaging Radiat Oncol* 2017; **61**: 394–401.
3. Padayachee J, Loh J, Tiong A, Lao L. National survey on image-guided radiotherapy practice in New Zealand. *J Med Imaging Radiat Oncol* 2018; **62**: 262–9.
4. Rybovic M, Banati RB, Cox J. Radiation therapy treatment verification imaging in Australia and New Zealand. *J Med Imaging Radiat Oncol* 2008; **52**: 183–90.
5. Australian Institute of Health and Welfare. Healthy Communities: Overweight and Obesity Rates Across Australia June 2018. AIHW, Canberra, ACT, 2018.
6. Wood TJ, Moore CS, Horsfield CJ, Saunderson JR, Beavis AW. Accounting for patient size in the optimization of dose and image quality of pelvis cone beam CT protocols on the Varian OBI system. *Br J Radiol* 2015; **88**: 20150364.
7. The Royal Australian and New Zealand College of Radiologists. Position Paper on Image Guided Radiation Therapy (IGRT) 2015. Australia The Royal Australian and New Zealand College of Radiologists, Sydney, NSW, 2015.
8. The Royal College of Radiologists. On Target: Ensuring Geometric Accuracy in Radiotherapy. The Royal College of Radiologists Society and College of Radiographers Institute of Physics and Engineering in Medicine, London, UK, 2008.
9. Yin F, Wong J, Balter J, et al. The Role of in-Room kV X-Ray Imaging for Patient Setup and Target Localization: Report of Task Group 104 of the Therapy Imaging Committee. American Association of Physicists in Medicine, College Park, MD, 2009.
10. World Health Organization. Obesity: Preventing and Managing the Global Epidemic. Report of a WHO Consultation. World Health Organisaton, Geneva, 2000.
11. Brown A, Tan A, Cooper S, Fielding A. Obesity does not influence prostate intrafractional motion. *J Med Radiat Sci* 2018; **65**: 31–8.
12. Rogers J, Welgemoed C, Gujral D. Does body mass index or subcutaneous adipose tissue thickness affect interfraction prostate motion in patients receiving radical prostate radiotherapy? *J Radiother Pract* 2016; **15**: 334–40.
13. National Health and Medical Research Council. Clinical Practice Guidelines for the Management of Overweight and Obesity in Adults, Adolescents and Children in Australia. Melbourne: Melbourne: National Health and Medical Research Council, 2013.
14. Varian Medical Systems. On-Board Imager (OBI) Advanced Imaging Reference Guide. Palo Alto, USA: Varian Medical Systems, 2013.
15. Leong A, Clarkson G, Lang S, Zamburlini M, Cavelaars F, Winter C. Practical optimisation of kV and CBCT imaging dose. *Radiother Oncol* 2014; **111**: S109.
16. Wallace D, Ng JA, Keall PJ, et al. Determining appropriate imaging parameters for kilovoltage intrafraction monitoring: An experimental phantom study. *Phys Med Biol* 2015; **60**: 4835–47.
17. Wallace D, Booth J, Aun J, Keall P, Poulsen P. Investigation of parameters affecting image quality for Kilovoltage Intrafraction Monitoring (KIM) during RapidArc prostate radiotherapy. *J Med Imaging Radiat Oncol* 2014; **58**: 164.
18. Carucci L. Imaging obese patients: Problems and solutions. *Abdom Imaging* 2013; **38**: 630–46.
19. Glanc P, O'Hayon BE, Singh DK, Bokhari SAJ, Maxwell CV. Challenges of pelvic imaging in obese women. *Radiographics* 2012; **32**: 1839–62.
20. Uppot RN, Sahani DV, Hahn PF, Gervais D, Mueller PR. Impact of obesity on medical imaging and image-guided intervention. *Am J Roentgenol* 2007; **188**: 433–40.
21. Pierce R. Perimeter of an Ellipse. 2017 [cited 2019 April 15]. Available from: https://www.mathsisfun.com/geometry/ellipse-perimeter.html.
22. Martin AD, Daniel MZ, Drinkwater DT, Clarys JP. Adipose tissue density, estimated adipose lipid fraction and whole body adiposity in male cadavers. *Int J Obes Relat Metab Disord* 1994; **18**: 79–83.
23. Mileto A, Ramirez-Giraldo JC, Nelson RC, et al. High-pitch dual-source MDCT for imaging of the thoracoabdominal aorta: Relationships among radiation dose, noise, pitch, and body size in a phantom experiment and clinical study. *Am J Roentgenol* 2015; **205**: 834–9.
24. Zhang LJ, Qi L, De Cecco CN, et al. High-pitch coronary CT angiography at 70 kVp with low contrast medium volume: Comparison of 80 and 100 kVp high-pitch protocols. *Medicine (United States)* 2014; **93**: e092.
25. Wolbarst AB. Physics of Radiology, 2nd edn. Medical Physics Publishing, Madison, WI, 2005.

26. Schindera ST, Nelson RC, Lee ER, et al. Abdominal multislice CT for obese patients: Effect on image quality and radiation dose in a phantom study. *Acad Radiol* 2007; **14**: 486–94.

27. Murphy MJ, Balter J, Balter S, et al. The management of imaging dose during image-guided radiotherapy: Report of the AAPM Task Group 75. *Med Phys* 2007; **34**: 4041–63.